

Communication: Tunnelling splitting in the phosphine molecule

Clara Sousa-Silva, Jonathan Tennyson, and Sergey N. Yurchenko

Citation: *The Journal of Chemical Physics* **145**, 091102 (2016); doi: 10.1063/1.4962259

View online: <http://dx.doi.org/10.1063/1.4962259>

View Table of Contents: <http://scitation.aip.org/content/aip/journal/jcp/145/9?ver=pdfcov>

Published by the **AIP Publishing**

Articles you may be interested in

First-principles calculations of rovibrational energies, dipole transition intensities and partition function for ethylene using MULTIMODE

J. Chem. Phys. **137**, 154301 (2012); 10.1063/1.4758005

Communications: Direct dynamics study of the $O(P^3) + C_2H_2$ reaction: Contribution from spin nonconserving route

J. Chem. Phys. **133**, 011101 (2010); 10.1063/1.3454727

Ab initio prediction of the infrared-absorption spectrum of the C_2Cl radical

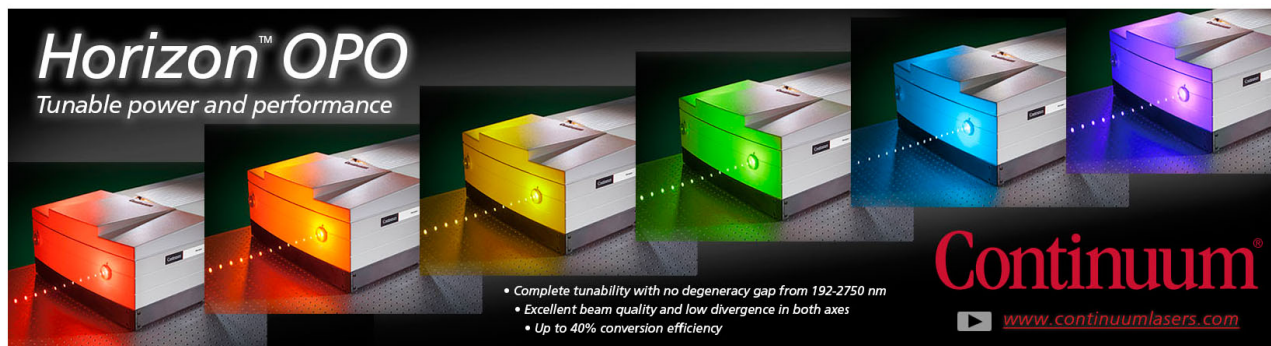
J. Chem. Phys. **123**, 014320 (2005); 10.1063/1.1950547

Vibrational spectra and intramolecular vibrational redistribution in highly excited deuterobromochlorofluoromethane CDBrClF: Experiment and theory

J. Chem. Phys. **113**, 2701 (2000); 10.1063/1.1302083

Vibrational spectroscopy of phosphaethyne (HCP). I. Potential energy surface, variational calculations, and comparison with experimental data

J. Chem. Phys. **112**, 8446 (2000); 10.1063/1.481483



Horizon™ OPO
Tunable power and performance

• Complete tunability with no degeneracy gap from 192-2750 nm
• Excellent beam quality and low divergence in both axes
• Up to 40% conversion efficiency

Continuum®
www.continuumlasers.com

The advertisement features a row of five Continuum Horizon OPO laser units, each emitting a different color of light: red, orange, yellow, green, and blue. The units are shown from a three-quarter perspective, highlighting their compact, rectangular design. The background is dark, making the glowing units stand out.

Communication: Tunnelling splitting in the phosphine molecule

Clara Sousa-Silva, Jonathan Tennyson, and Sergey N. Yurchenko

Department of Physics and Astronomy, University College London, London WC1E 6BT, United Kingdom

(Received 13 July 2016; accepted 16 August 2016; published online 6 September 2016)

Splitting due to tunnelling via the potential energy barrier has played a significant role in the study of molecular spectra since the early days of spectroscopy. The observation of the ammonia doublet led to attempts to find a phosphine analogous, but these have so far failed due to its considerably higher barrier. Full dimensional, variational nuclear motion calculations are used to predict splittings as a function of excitation energy. Simulated spectra suggest that such splittings should be observable in the near infrared via overtones of the ν_2 bending mode starting with $4\nu_2$. *Published by AIP Publishing*. [<http://dx.doi.org/10.1063/1.4962259>]

The umbrella mode in ammonia provides a textbook example of tunnelling splitting.¹ That the inversion of pyramidal NH_3 should lead to an observable splitting of the energy levels was first theoretically predicted in 1932² and then detected using microwave spectroscopy in 1934.³ The subtle effects of this tunnelling on the energy levels of ammonia are now well-studied.⁴ As a direct analogue of ammonia, phosphine can also be expected to display splitting of its energy levels due to the tunnelling effect. However, splitting in PH_3 is yet to be observed, despite multiple attempts spread over more than 80 years.^{5–11} Although otherwise similar to ammonia, phosphine has a larger mass and a much higher and wider barrier which makes for a much smaller splitting of the energy levels.¹ *Ab initio* calculations of the energy barrier for phosphine range from $12\,270\text{ cm}^{-1}$ to $12\,560\text{ cm}^{-1}$,¹² while the only empirical estimate gave a slightly lower value of $11\,030\text{ cm}^{-1}$.¹³

Experimentally, the infrared spectrum of PH_3 has been well studied (see Table 1 of Sousa-Silva *et al.*¹⁴ and the recent study by Malathy Devi *et al.*¹⁵). While most of this work has concentrated on the region below 3500 cm^{-1} , where our calculations suggest the tunnelling splitting is very small, Ulenikov *et al.*¹⁶ report observed spectra between 1750 and 9200 cm^{-1} and clearly demonstrate that PH_3 spectra can be observed at higher frequencies.

Of all the possible phosphine modes, the tunnelling effect should be most prominent in the symmetric bending mode, ν_2 , as it is the mode most strongly associated with the height of the pyramid formed with the phosphorous atom on top. In ammonia the analogous ν_2 mode is known as the inversion mode. Figure 1 shows schematically the relationship between this mode and the barrier to tunnelling for the phosphine molecule.

The ExoMol group works on constructing comprehensive line lists for modelling the atmospheres of hot bodies such as cool stars and exoplanets.¹⁷ As part of this work, we have computed two line lists for $^{31}\text{PH}_3$ in its ground electronic state.^{14,18} The more accurate of these line lists, called SAITY,¹⁸ contains 16×10^9 transitions between 9.8×10^6 energy levels and it is suitable for simulating spectra up to temperatures of 1500 K . It covers wavenumbers up to $10\,000\text{ cm}^{-1}$ and

includes all transitions to upper states with energies below $hc \cdot 18\,000\text{ cm}^{-1}$ and rotational excitation up to $J = 46$.

The PH_3 line lists were computed by the variational solution of the Schrödinger equation for the rotation-vibration motion employing the nuclear-motion program TROVE.¹⁹ The line lists were computed using $C_{3v}(M)$ symmetry, considering phosphine as a rigid molecule and thus with the potential barrier between the two symmetry-equivalent minima effectively set to infinity. Consequently, it originally neglected the possibility of a tunnelling mode.

Tunnelling can be considered as a chemical reaction and as such it is very sensitive to the shape of the potential energy surface (PES).¹ The SAITY line list used a spectroscopically refined version of the *ab initio* (CCSD(T)/aug-cc-pV(Q+d)Z) potential energy surface (PES).²⁰ The value of splitting in various vibrational states as well as the intensity of the inversion-rotation and inversion-ro-vibrational lines can be computed by adapting the procedure used to simulate the phosphine spectrum to work with $D_{3h}(M)$ symmetry. $D_{3h}(M)$ is the permutation inversion group for ammonia, since it is much less rigid molecule than phosphine.

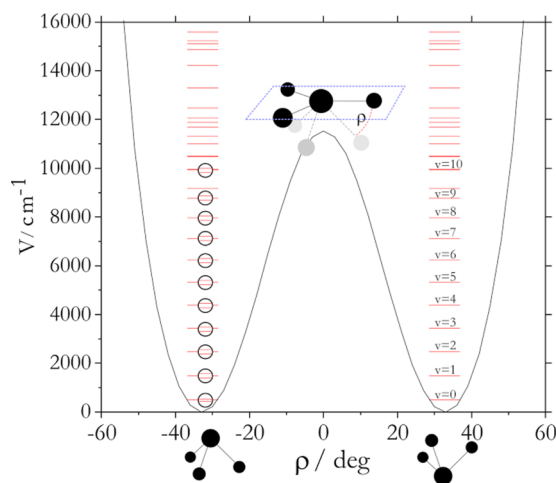


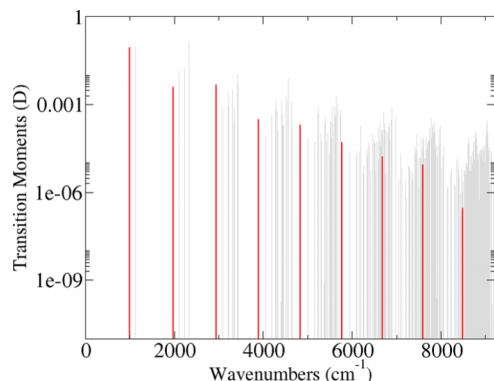
FIG. 1. Splitting of the energy levels for phosphine, showing the splitting for the ground state and the vibrational excitations up to $\nu = 10$ in the bending band ν_2 .

TABLE I. Calculated splitting for the ground state (GS), fundamental, and excited bands of the bending mode ν_2 .

Band	Energy ¹⁸	Splitting (cm ⁻¹)
GS	0.000	$\leq 10^{-10}$
ν_2	992.136	2×10^{-8}
$2\nu_2$	1972.576	6×10^{-7}
$3\nu_2$	2940.810	1×10^{-5}
$4\nu_2$	3895.685	0.0001
$5\nu_2$	4837.223	0.0009
$6\nu_2$	5767.008	0.0028
$7\nu_2$	6687.601	0.0165
$8\nu_2$	7598.124	0.0525
$9\nu_2$	8494.683	0.6243

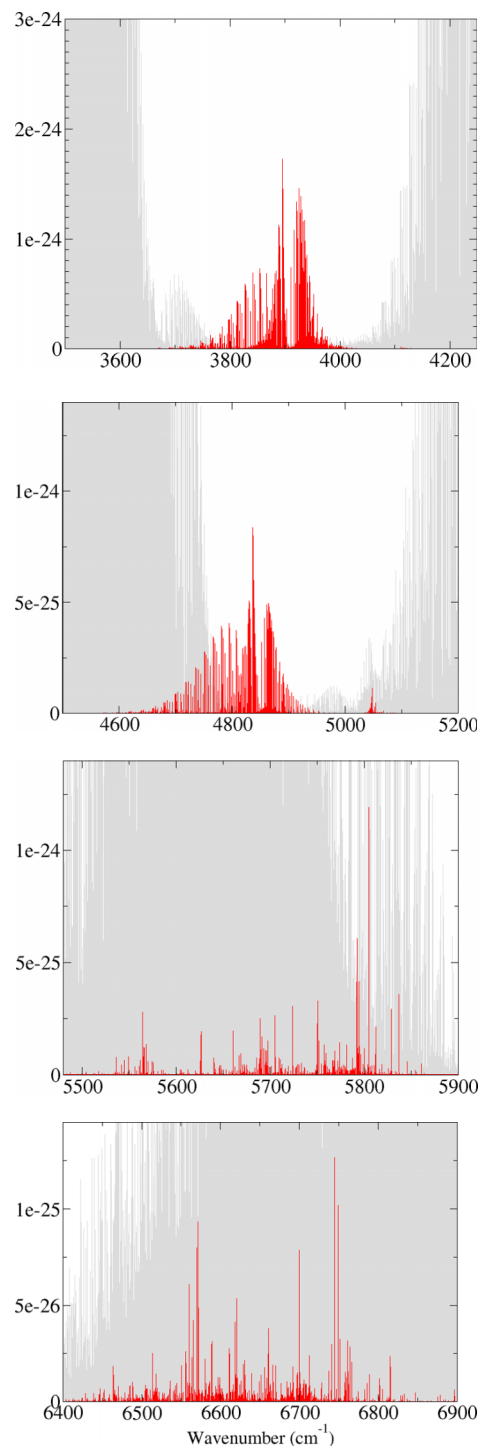
TROVE is used to compute differences between split energy levels. Here we employ the same refined PES as that used to compute the SAITY line list to predict the splitting between states of A'_1 and A''_2 symmetry for $J = 0$, considering a zero point energy of 5232.26 cm^{-1} . The potential energy function and the kinetic energy operator are expanded (six and eight orders, respectively) in terms of the five non-linearized internal coordinates (three stretching and two deformational bending) around a symmetric one-dimensional non-rigid reference configuration represented by the inversion mode. The vibrational basis functions are obtained in a two-step contraction approach as described by Yurchenko *et al.*²¹ The stretching (ν_1 and ν_3) primitive basis function $|v_{\text{str}}\rangle$ ($v_{\text{str}} = 0 \dots 7$) is obtained using the Numerov-Cooley method.^{22,23} Harmonic oscillators are used as basis functions for the bending (ν_4) primitive, $|v_{\text{bend}}\rangle$ ($v_{\text{bend}} = 0 \dots 24$). For the ν_2 inversion mode, primitive basis functions, $|v_{\text{inv}}\rangle$, are used. These were also generated with the Numerov-Cooley method, with $v_{\text{inv}} \leq 64$.

The phosphine barrier height values used in the TROVE input were $11\,130.0 \text{ cm}^{-1}$ for the planar local minimum with P–H bonds at 1.3611 \AA , refined from an *ab initio* value of $113\,53.6 \text{ cm}^{-1}$ for the local minimum at 1.3858 \AA . Both the *ab initio* and refined barrier heights are extrapolated values from the potential parameters in the PES. These values are somewhat lower than the previous, lower-level *ab initio*

FIG. 2. Transition moments (Debye, log scale) for excitations from the ground vibrational states up to $16\,000 \text{ cm}^{-1}$. Transitions associated with ν_2 mode excitations are highlighted.

estimates but are in reasonable agreement with the empirical estimate of Weston.¹³

To help assess the uncertainty in our predicted splittings, calculations were made using two different PES surfaces, pre- and post-refinement, corresponding to the surfaces used to calculate the phosphine line list at room temperature¹⁴ and the complete SAITY line list,¹⁸ respectively. Even though the refined PES resulted in a significant improvement in the

FIG. 3. Contrast between the (top to bottom) $4\nu_2$, $5\nu_2$, $6\nu_2$, and $7\nu_2$ bands and the neighbouring transitions at $T = 296 \text{ K}$. The SAITY absorption intensities (cm/molecule) are computed using a $C_{3v}(M)$ model with PH_3 as a rigid molecule, i.e., neglecting the inversion splitting.¹⁸

accuracy of the overall phosphine line list, the predicted splittings agreed completely up to four significant figures.

Table I shows how the predicted splittings change as a function of ν_2 excitation. Splittings in the ground state are known to be extremely small¹² (our calculations suggest about 10^{-10} cm⁻¹) but increase significantly as the ν_2 mode is excited. All splitting predictions are converged to within 40% up to $7\nu_2$; use of even larger inversion basis sets ($v_{\text{inv}} > 64$) became numerically unstable.

Our tunnelling splitting for the overtones of ν_2 is somewhat larger than those predicted by previous one-dimension studies.^{10,12} This could have been anticipated as it is well-known²⁴ that the treatment of tunnelling which considers all dimensions of the problem leads to increases in the magnitude of the splitting (or faster tunnelling). Additionally, our lower value for the barrier height also contributes to the larger predicted splitting values.

Any observation of the tunnelling splitting in PH₃ has to consider a number of factors. First, this splitting has to be distinguished from the hyperfine structure. The hyperfine splitting in PH₃ has been observed^{25,26} to be less than 1 MHz or 4×10^{-5} cm⁻¹ and should not increase significantly

with vibrational excitation. Consequently, the splitting due to inversion should be distinguishable from the hyperfine splitting for all bands associated with vibrational excitation to $4\nu_2$ and higher. Besides, the nuclear statistics of PH₃ as a D_{3h}(M) symmetry molecule should be also taken into account. For example, as in the case of NH₃, the ro-vibrational states of the A'_1 and A''_1 symmetries have zero nuclear statistical weights g_{ns} and thus forbidden, with $g_{\text{ns}} = 8, 8, 4,$ and 4 for $A'_2, A''_2, E',$ and E'' , respectively.

Due to their reasonably large energy splittings, promising regions of possible detection are those of the symmetric bending bands, $6\nu_2$ (≈ 5800 cm⁻¹) and $7\nu_2$ (≈ 6700 cm⁻¹). Their splittings are predicted to be approximately 0.003 cm⁻¹ and 0.02 cm⁻¹ for $6\nu_2$ and $7\nu_2$, respectively. Our calculations suggest that most intense lines in this band have intensities of about 10^{-24} cm/molecule at $T = 296$ K and should be easily observable with modern instruments. Figure 2 summarises the dipole transition moments to various vibrational states from the vibrational ground state; transitions to the ν_2 overtone series associated with the tunnelling motion are highlighted.

However, detection will also depend on the location of the splitting transitions as it may be difficult to distinguish the ν_2 bands in regions of the spectrum that are strongly populated by other bands. Figure 3 highlights the spectroscopic regions

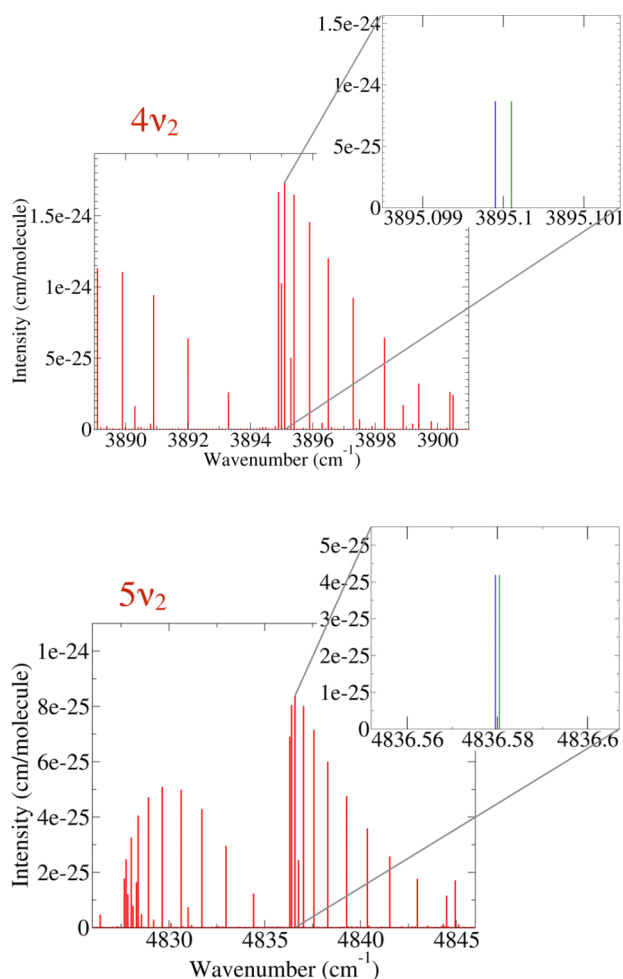


FIG. 4. Comparison between predicted phosphine spectra without (red) and with (blue and green) the inclusion of tunnelling motion, for the strongest transitions in the $4\nu_2$ and $5\nu_2$ overtone bands. The ro-vibrational splitting is estimated using the pure vibrational values from Table I. The SAITY line list is used to simulate absorption intensities for a temperature of 296 K.

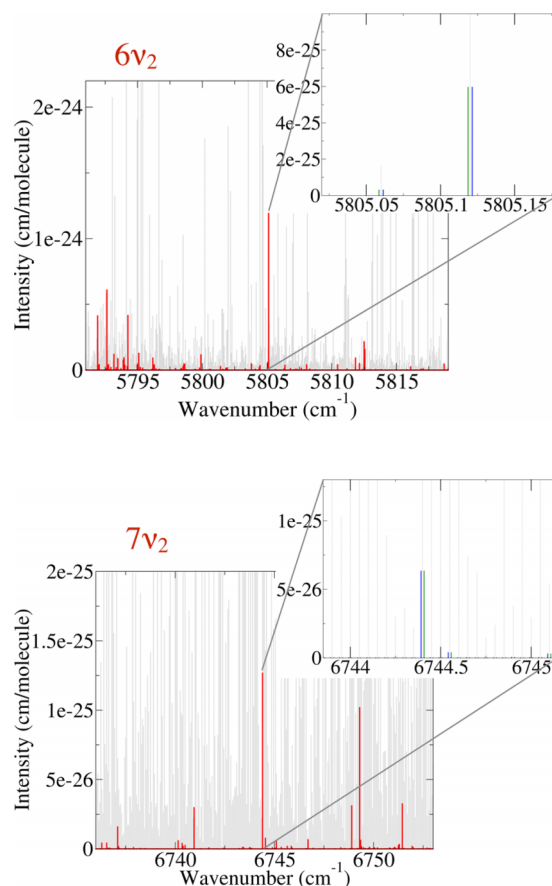


FIG. 5. Comparison between predicted phosphine spectra without (red) and with (blue and green) the inclusion of tunnelling motion, for the strongest transitions in the $6\nu_2$ and $7\nu_2$ overtone bands. The ro-vibrational splitting is estimated using the pure vibrational values from Table I. The SAITY line list is used to simulate absorption intensities for a temperature of 296 K.

where splitting could be detected in the context of the surrounding spectrum for the $4\nu_2$, $5\nu_2$, $6\nu_2$, and $7\nu_2$ bands. In this context, the positions of the $4\nu_2$ and $5\nu_2$ bands appear to be particularly promising for investigation, since they can be mostly isolated from the surrounding stronger bands.

Figure 4 shows the predicted spectra in the region of the strongest transitions for $4\nu_2$ and $5\nu_2$ bands, comparing spectra when the molecule is allowed to undergo inversion and when tunnelling is not permitted. Additionally, Figure 5 shows how the $6\nu_2$ and $7\nu_2$ bands will be harder to detect amongst the surrounding bands, despite having much larger splitting values.

Our calculations show that the ν_2 overtones display splittings of a magnitude that should be resolvable with modern experiments. We therefore hope that the theoretical predictions of phosphine tunnelling shown here will be validated with experimental detection in the near future. Simulated spectra for other regions and/or conditions can be provided by the authors to aid this process.

This work is supported by ERC Advanced Investigator Project No. 267219. We would like to thank Oleg Polyansky, Laura McKemmish, Ahmed Al-Refaie, Jack D. Franklin, and William Azubuikwe for their support and advice.

¹R. P. Bell, *The Tunnel Effect in Chemistry* (Springer, 1980), pp. 51–76.

²D. M. Dennison and G. E. Uhlenbeck, *Phys. Rev.* **41**, 313 (1932).

³C. E. Cleeton and N. H. Williams, *Phys. Rev.* **45**, 234 (1934).

⁴A. G. Csaszar and T. Furtenbacher, *Phys. Chem. Chem. Phys.* **18**, 1092 (2016).

⁵N. Wright and H. M. Randall, *Phys. Rev.* **44**, 391 (1933).

⁶R. E. Stroup, R. A. Oetjen, and E. E. Bell, *J. Opt. Soc. Am.* **43**, 1096 (1953).

⁷P. Helminger and W. Gordy, *Phys. Rev.* **188**, 100 (1969).

⁸P. B. Davies, R. M. Neumann, S. C. Wofsy, and W. Klemperer, *J. Chem. Phys.* **55**, 3564 (1971).

⁹A. G. Maki, R. L. Sams, and W. B. Olson, *J. Chem. Phys.* **58**, 4502 (1973).

¹⁰V. Špirko and D. Papoušek, *Mol. Phys.* **36**, 791 (1978).

¹¹S. P. Belov, A. V. Burenin, L. I. Gershtein, A. F. Krupnov, V. N. Markov, A. V. Maslovsky, and S. M. Shapin, *J. Mol. Spectrosc.* **86**, 184 (1981).

¹²P. Schwerdtfeger, L. J. Laakkonen, and P. Pyykkö, *J. Chem. Phys.* **96**, 6807 (1992).

¹³R. E. Weston, Jr., *J. Am. Chem. Soc.* **76**, 2645 (1954).

¹⁴C. Sousa-Silva, S. N. Yurchenko, and J. Tennyson, *J. Mol. Spectrosc.* **288**, 28 (2013).

¹⁵V. Malathy Devi, I. Kleiner, R. L. Sams, L. R. Brown, D. C. Benner, and L. N. Fletcher, *J. Mol. Spectrosc.* **298**, 11 (2014).

¹⁶O. N. Ulenikov, E. S. Bekhtereva, V. A. Kozinskaia, J. J. Zheng, S. G. He, S. M. Hu, Q. S. Zhu, C. Leroy, and L. Pluchart, *J. Mol. Spectrosc.* **215**, 295 (2002).

¹⁷J. Tennyson and S. N. Yurchenko, *Mon. Not. R. Astron. Soc.* **425**, 21 (2012).

¹⁸C. Sousa-Silva, A. F. Al-Refaie, J. Tennyson, and S. N. Yurchenko, *Mon. Not. R. Astron. Soc.* **446**, 2337 (2015).

¹⁹S. N. Yurchenko, W. Thiel, and P. Jensen, *J. Mol. Spectrosc.* **245**, 126 (2007).

²⁰R. I. Ovsyannikov, W. Thiel, S. N. Yurchenko, M. Carvajal, and P. Jensen, *J. Chem. Phys.* **129**, 044309 (2008).

²¹S. N. Yurchenko, R. J. Barber, and J. Tennyson, *Mon. Not. R. Astron. Soc.* **413**, 1828 (2011).

²²B. Noumeroff, “Méthode nouvelle de la détermination des orbites et le calcul des éphémérides en tenant compte des perturbations,” in *Trudy Glavnoi Rossiiskoi Astrofizicheskoi Observatorii* (Gosudarstvennoe Izdatel'stvo, Moscow, 1923), Vol. 2, pp. 188–259.

²³J. W. Cooley, *Math. Comput.* **15**, 363 (1961).

²⁴W. Klopper, M. Quack, and M. A. Suhm, *Chem. Phys. Lett.* **261**, 35 (1996).

²⁵H. S. P. Müller, *J. Quant. Spectrosc. Radiat. Transfer* **130**, 335 (2013).

²⁶G. Cazzoli and C. Puzzarini, *J. Mol. Spectrosc.* **239**, 64 (2006).